Earth, Planets and Space
a SpringerOpen Journal

FULL PAPER　　　　　　　　　　　　　　　　　　　　　　　　**Open Access**

Evolutionary process of Beppu Bay in central Kyushu, Japan: a quantitative study of the basin-forming process controlled by plate convergence modes

Yasuto Itoh[1*], Shigekazu Kusumoto[2] and Keiji Takemura[3]

Abstract

This integrated tectonic study reveals the basin-forming and deforming processes on an active margin. Southwest Japan (SWJ) is an island arc under the influence of oblique subduction of the Philippine Sea plate, which has provoked dextral slips on the arc-bisecting Median Tectonic Line (MTL). Plio-/Pleistocene sediments in Beppu Bay, a tectonic depression at the westernmost portion of the MTL, are categorized into lower (5 ~ 0.7 Ma), upper (0.7 ~ 0.3 Ma), and an auxiliary uppermost (0.3 Ma ~ present) unit in ascending order. Detailed seismic interpretation demonstrates that major structures in the deep interior of the basin are an older half-graben under a strong N-S extensional regime and a younger pull-apart sag that developed in a right-stepping part of the MTL as a result of late Quaternary-enhanced strike-slip rates on the fault. Sediments within the pull-apart have been deformed by later inversion events as a contraction phase arose. Conspicuous deformation of the hanging wall of the low-angle detachment of the basin was successfully reproduced by numerical modeling. Based on a discrete element method, this suggests that structural differences in the deformed sedimentary layers are caused by differences in the dip angles of the faults. Remarkable temporal changes in tectonic regimes around Beppu Bay and other areas of SWJ are probably related to transient modes of convergence, including the migration of the Euler pole, of the Philippine Sea plate since ca. 6 Ma.

Keywords: Beppu Bay; Kyushu; Southwest Japan; Seismic interpretation; Numerical modeling; Philippine Sea plate; Oblique subduction; Transcurrent fault; Pull-apart basin; Inversion
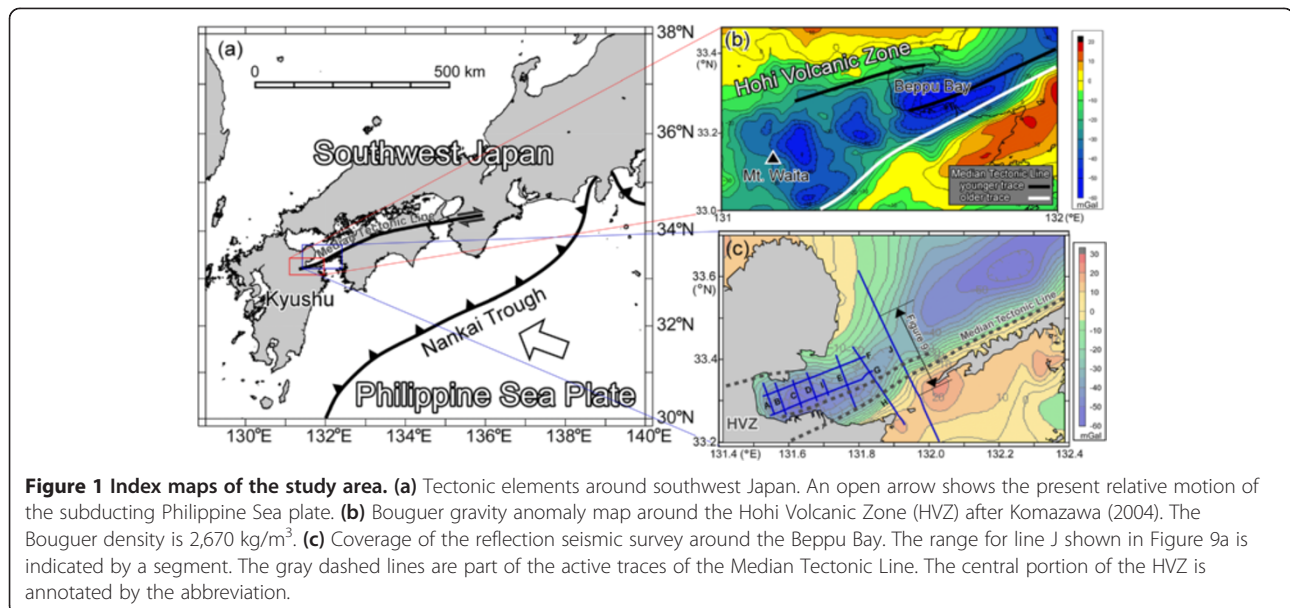
Background

Subduction of oceanic plates results in deformation of continental margins and formation of various tectonic basins. A recent synthesis of the basin architecture of active plate margins (Itoh 2013) revealed that the modes of plate convergence (subduction rate, obliquity, slab steepness, etc.) play a crucial role in determining basin evolution patterns (e.g., Itoh et al. 2014; Takano et al. 2013). In other words, spatial/temporal variations in sedimentary basin morphology on an active margin give clues to changes in the convergence modes of oceanic plates and to regional tectonic history.

Beppu Bay (Figure 1), located in central Kyushu in southwest Japan (hereafter referred to as SWJ), is a typical example of a tectonically controlled sedimentary basin under the influence of the Philippine Sea plate convergence. A tension graben, the Hohi Volcanic Zone (Figure 1; hereafter referred to as the HVZ), which includes the Beppu Bay, emerged in central Kyushu at ca. 5 Ma (Itoh et al. 1998) accompanying vigorous volcanism. The evolutionary process of the HVZ has been controlled by the activity of a large bisecting fault in SWJ, namely, the Median Tectonic Line (hereafter referred to as the MTL). Changes in the obliquity of the Philippine Sea plate motion have provoked thrusting and dextral slips on the MTL, which initiated as a regional crustal break in the Cretaceous east Eurasian margin and whose active segment has shrunk during the late Quaternary as suggested by geomorphological features (Research Group for Active

* Correspondence: yasutokov@yahoo.co.jp
[1]Graduate School of Science, Osaka Prefecture University, Osaka 599-8531, Japan
Full list of author information is available at the end of the article

Springer

Figure 1 Index maps of the study area. (a) Tectonic elements around southwest Japan. An open arrow shows the present relative motion of the subducting Philippine Sea plate. **(b)** Bouguer gravity anomaly map around the Hohi Volcanic Zone (HVZ) after Komazawa (2004). The Bouguer density is 2,670 kg/m³. **(c)** Coverage of the reflection seismic survey around the Beppu Bay. The range for line J shown in Figure 9a is indicated by a segment. The gray dashed lines are part of the active traces of the Median Tectonic Line. The central portion of the HVZ is annotated by the abbreviation.

Faults 1991). The MTL acted as a listric fault of the Neogene incipient half-graben of the HVZ. Itoh et al. (1998) described a process migration of the depocenters in the HVZ, among which the Beppu Bay is the youngest area of active subsidence.

The present study aims at quantitatively evaluating tectonic basin development, namely, visualizing geologic structures in 3D utilizing seismic reflection data with age control, and constructing a chronicle of tectonic deformation along the convergent margin. Our study area, the Beppu Bay, serves as an ideal example of tectonic basin development with various geological and geophysical datasets.

Kyushu Island, in the western part of the Japanese archipelago, is studded by numerous volcanoes that are an evidence of slab-induced magmatism, sporadic mantle upwelling, and fissure eruption upon deep tectonic ruptures. The HVZ is located in the central part of Kyushu and constitutes a large composite volcanic edifice, present since ca. 5 Ma. Itoh et al. (1998) categorized the HVZ components into older fissure volcanics filling a graben under N-S tensile stress and younger tholeiitic central eruptions controlled by regional fault activity. They also demonstrated that major depocenters in the HVZ, which are depicted as negative parts in the Bouguer anomaly maps in Figure 1, migrated eastward under transient (tensional to transtensional/transpressional) tectonic stress. The structural framework of the older western (onshore) segment of the HVZ has been described based on many drilling surveys, whereas the younger eastern (offshore) depression around Beppu Bay has not been fully studied because of scarce subsurface information.

Quantitative analysis of tectonic basin formation has been undertaken by Kusumoto et al. (1999). Based on dislocation modeling, they successfully restored the formation and migration process of depocenters within the HVZ assuming subduction-driven slips on a minimum number of faults. Among them, the MTL played an important role in forming an active depression around the Beppu Bay according to changes in its active trace. The subsurface structure predicted by the numerical modeling should be verified by means of a seismic reflection survey.

A pioneering seismic study by Yusa et al. (1992) described low-angle faults at the bottom of the HVZ parallel to the basin's long axis and a rollover structure at the center of the bay creating a sharp contrast of basin morphology. Although their findings are essential structural components in the study area, they did not recognize continuous reflectors in basin-filling sediments, which are linked to tectonic and/or eustatic processes. As a result, their significant study was rather lacking in its ability to distinguish temporal shifts in the structural styles of the extensive basin and related regional stress regimes. Based on the morphology of an intra-basin seismic horizon, Itoh et al. (1998) argued that development of the active depression was divided into an incipient tensional stage and succeeding transtensional/transpressional stages related to enhanced dextral slips on the MTL. They found that the morphology of the so-called flower structure (Harding 1990) on N-S seismic profiles is indicative of a transition of active strike-slip segments on the MTL. However, their analysis was concentrated around the mouth of the bay, and the structural style of the inner Beppu Bay was out of the scope of their study.

Recently, Itoh et al. (2013a) pursued spatiotemporal transition of the deformation front in the bay under the influence of changes in MTL activity. Itoh et al. (2013b) gave an estimate of the total volume of the HVZ based on gravimetric analyses. However, their main focus was set on a large variety of tectonic styles along the active MTL trace. A comprehensive seismic interpretation integrating all the subsurface information has not yet been executed on the tectonic depression. That is the main purpose of the present study.

Methods

Interpretation of seismic reflection profiles

Data acquisition and processing

In 1989, an offshore seismic survey was conducted around Beppu Bay by Kyoto University. During the shooting of 138-km seismic lines (A to I in Figure 1c), 24 channels of hydrophones (at 25-m intervals) recorded the energy released from a 9.8-l (600 in.[3]) tuned air gun array, shot at 25-m intervals. Raw seismic data were stacked and then subjected to a post-stack processing sequence in order to enhance the resolution.

In 1990, Kyoto University conducted another offshore seismic survey around the Bungo Strait. During the shooting of a seismic line as long as 100 km (J in Figure 1c), 48 channels of hydrophones (at intervals of 26.66 m) recorded the energy released from a 36.9-l (2,250 in.[3]) tuned air gun array, shot at 26.66-m intervals. As for the previous survey, raw seismic data were stacked and then subjected to a post-stack processing sequence in order to enhance the resolution. Conversion from the two-way travel time to depth was done based on velocity analysis using the constant velocity stack method. The latest results of processing the data were presented by Abe et al. (2013). They reprocessed the seismic data of line J using algorithms for multiple suppression.

Characteristics of seismic reflection

Figure 2 (profile of line B) presents typical reflection characteristics of seismic profiles within the Beppu Bay. We identified three seismic markers, namely the purple, yellow, and cyan horizons, in ascending order. The lowermost purple horizon coincides with the top of the acoustic basement units. The purple horizon delineates a large depression around Beppu Bay. Basin-filling strata are roughly divided into a lower unit showing discontinuous or chaotic reflections and an upper unit accompanied with transparent and/or thinly laminated continuous reflection patterns. The yellow horizon is a discontinuous/continuous reflection boundary, which can be traced throughout the whole Beppu Bay. The uppermost cyan horizon is an auxiliary seismic reflector, which is recognized as a boundary between discontinuous strong reflections (lower) and continuous reflections (upper) onlapping the horizon, exclusively identified within the northwestern part of the bay.

Age assignment of reflectors

The geologic context around central Kyushu implies that pre-Neogene accretionary complexes (metamorphosed) and voluminous plutonic rocks constitute the majority of the acoustic basement, the top of which is depicted as the purple horizon in the present seismic interpretation. Thick clastics began to accumulate upon the erosion surface of the acoustic basement at ca. 5 Ma (e.g., Kamata 1989; Sasada 1987).

As no deep drilling survey has ever been conducted in the bay area, the authors attempted to correlate traceable seismic horizons with conspicuous geologic events based on surface and underground geologic surveys for the surrounding land areas like the stratigraphic synthesis by Ishizuka et al. (2005). First, we interpret the discontinuous/continuous reflection boundary as the unconformity between the Sekinan Group and the Oita Group. The former ranges between 2 and 1 Ma and consists of non-marine clastics intercalating abundant volcaniclastic rocks, whereas the latter includes pyroclastic flow deposits and non-marine to marine sediments, the base of which (the yellow horizon) is assigned to ca. 0.7 Ma.

The confined cyan horizon is interpreted as the top of the Hiji volcano, buried by fine sediments, part of which is exposed along the north coast of the Beppu Bay and dated to around 0.3 Ma based on the K-Ar method (Ishizuka et al. 2005).

Structural interpretation and volumetric analysis

Around Beppu Bay, countless surface ruptures have been found and described based on sounding surveys. Ishizuka et al. (2005) summarized these. Although they form a unique geomorphic province, identifying seismogenic faults and interpreting the tectonic condition should be based on fault morphology in the deep interior of the basin through the use of multi-channel reflection seismic data. In this section, we describe the structural components of the seismic profiles and submit a three-dimensional structural model of the conspicuous basin.

The structural characteristics of the N-S seismic profiles are presented in Figure 3 (line E). The lower seismic unit (purple-yellow interval) is thickest along the southern margin of the bay. It is controlled by the evolution of the asymmetric half-graben on the basal drag fault. On the other hand, the depocenter of the upper unit (yellow-sea bottom interval) is located in the northern part of the basin, and the surface of the yellow horizon dips toward the north. These features may infer that the top of the acoustic basement (purple horizon) acted as a slip surface during the deposition of the upper unit.
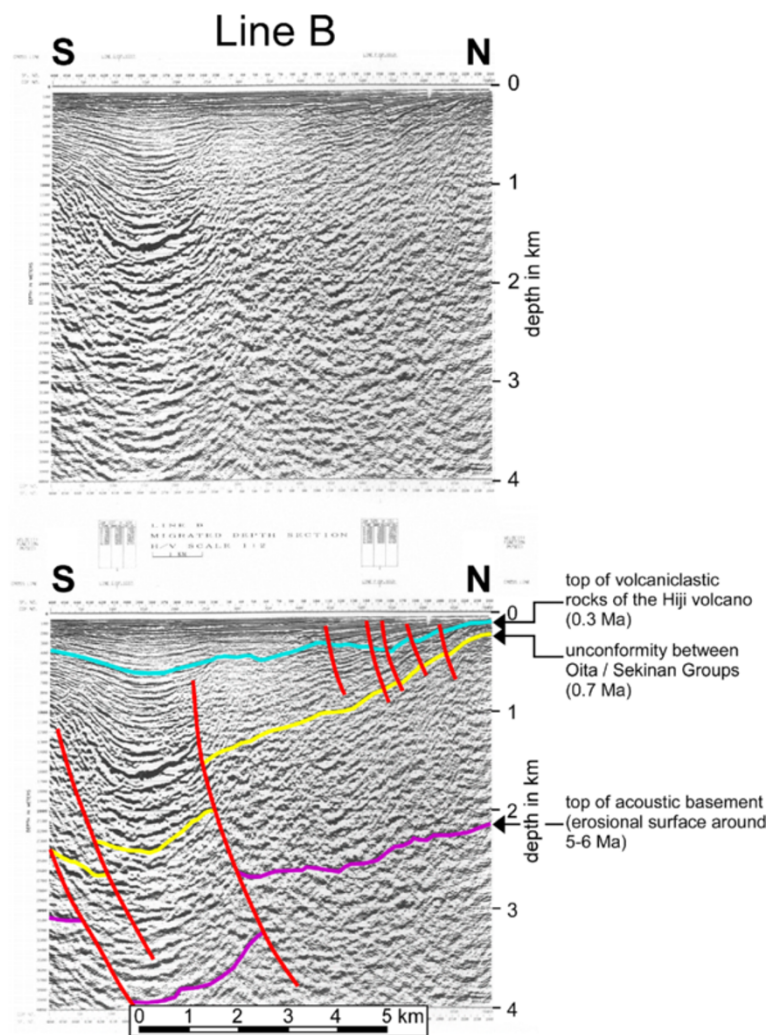
Figure 2 Seismic characteristics and stratigraphic interpretation of seismic horizons on line B (top, raw section; bottom, interpreted). See Figure 1 for line location. Vertical exaggeration (*V/H*) = 2.0.

The basin infill is studded by many high-angle faults, whose active parts seem to migrate northerly. Some faults on the northern flank of the Beppu Bay basin reach the surface of the infill and exhibit clear flower structures suggestive of active transcurrent faulting. Itoh et al. (1998) interpreted the spatiotemporal changes in the fault activity as transitions of active segments of the MTL. Using dislocation modeling, Kusumoto et al. (1999) showed that the right-stepping pattern of the MTL developed pull-apart basins at fault terminations, which collectively formed an extensive depression in the HVZ.

Figure 4 (line G running parallel to the younger trace of the MTL) delineates structural features on E-W seismic profiles. The most remarkable component is a bay-central rollover fault that emerged in a right-stepping part of the younger MTL (Figure 1b). To the east of the rollover, there are bunches of normal active faults constituting collapsed anticlines, which are developed along the younger trace of the MTL. The hanging wall on the west of the rollover has suffered later inversion, and the subsidence rate of the tectonic pull-apart tends to have lessened during the deposition of the upper unit. A contractional episode in the late Quaternary was also advocated from the viewpoint of volcanism on land. The form of eruption of volcanic rocks around the Mt. Waita area (Figure 1b) changed at about 0.7 Ma from lava plateaus to lava domes accompanied by a few stratovolcanoes. Kamata et al. (1988) explained this as resulting from local compressive stress loaded around Mt. Waita.

Figures 5, 6, 7 are isochron structural maps based on the present seismic interpretation. Figure 5 shows the top of the acoustic basement. The structure beyond
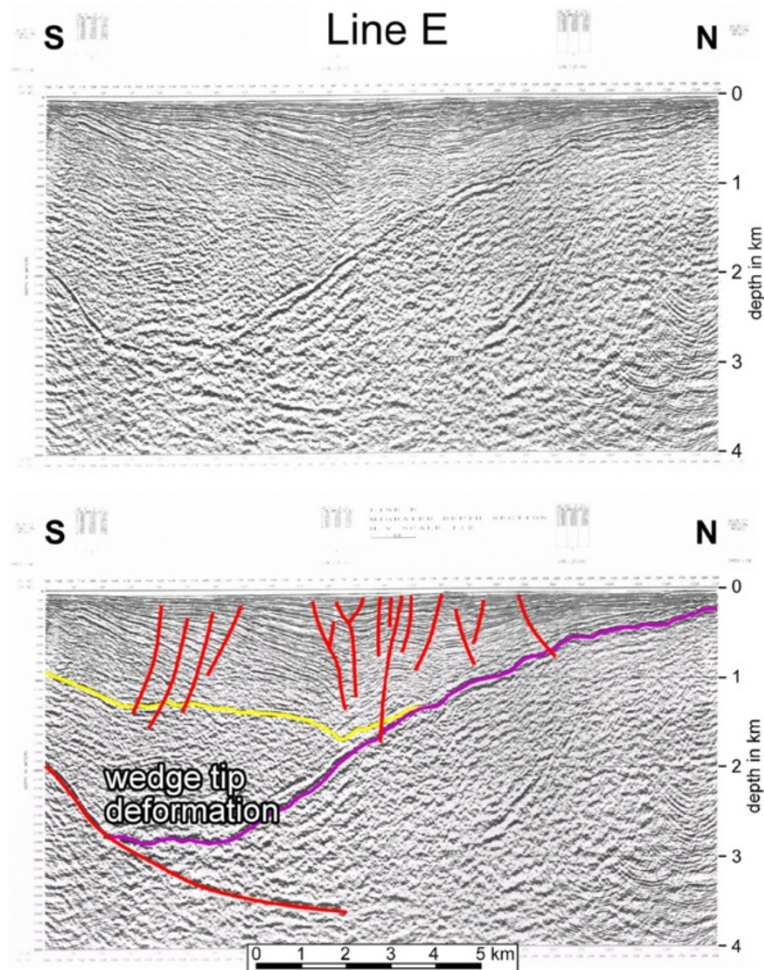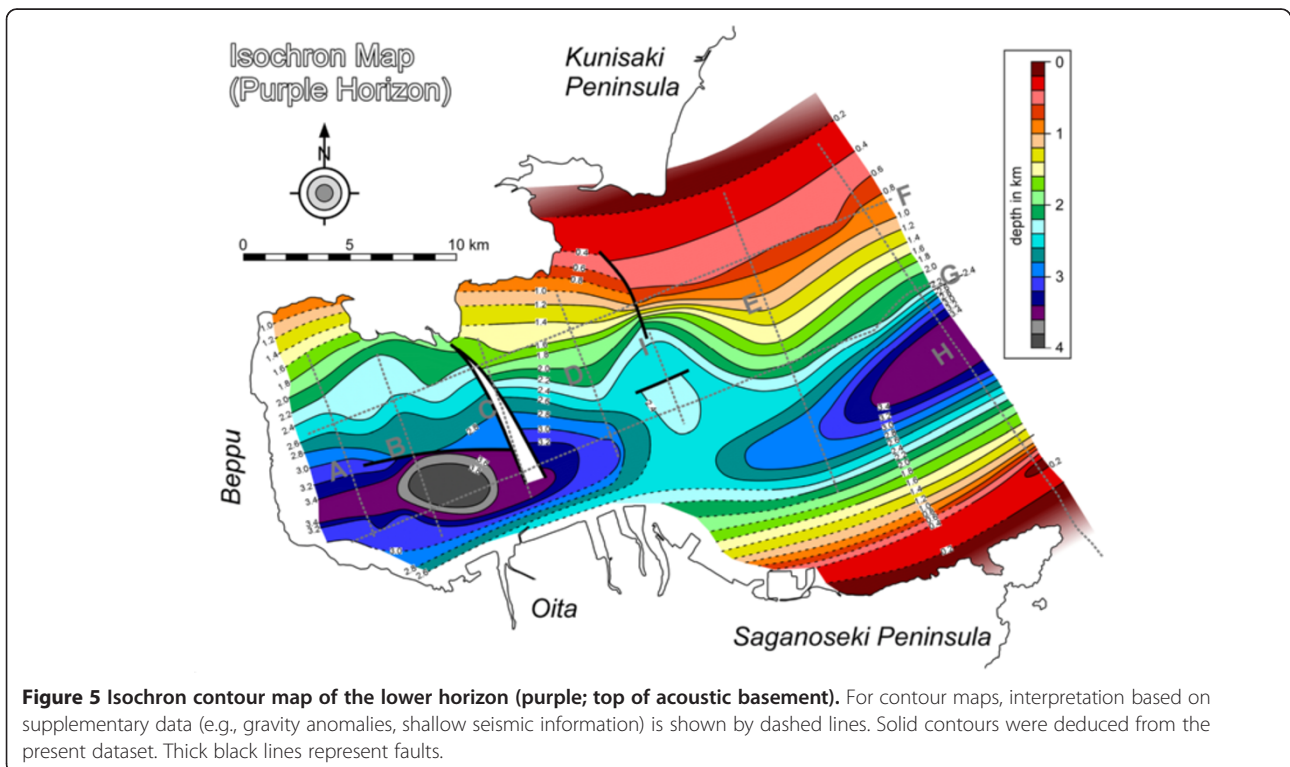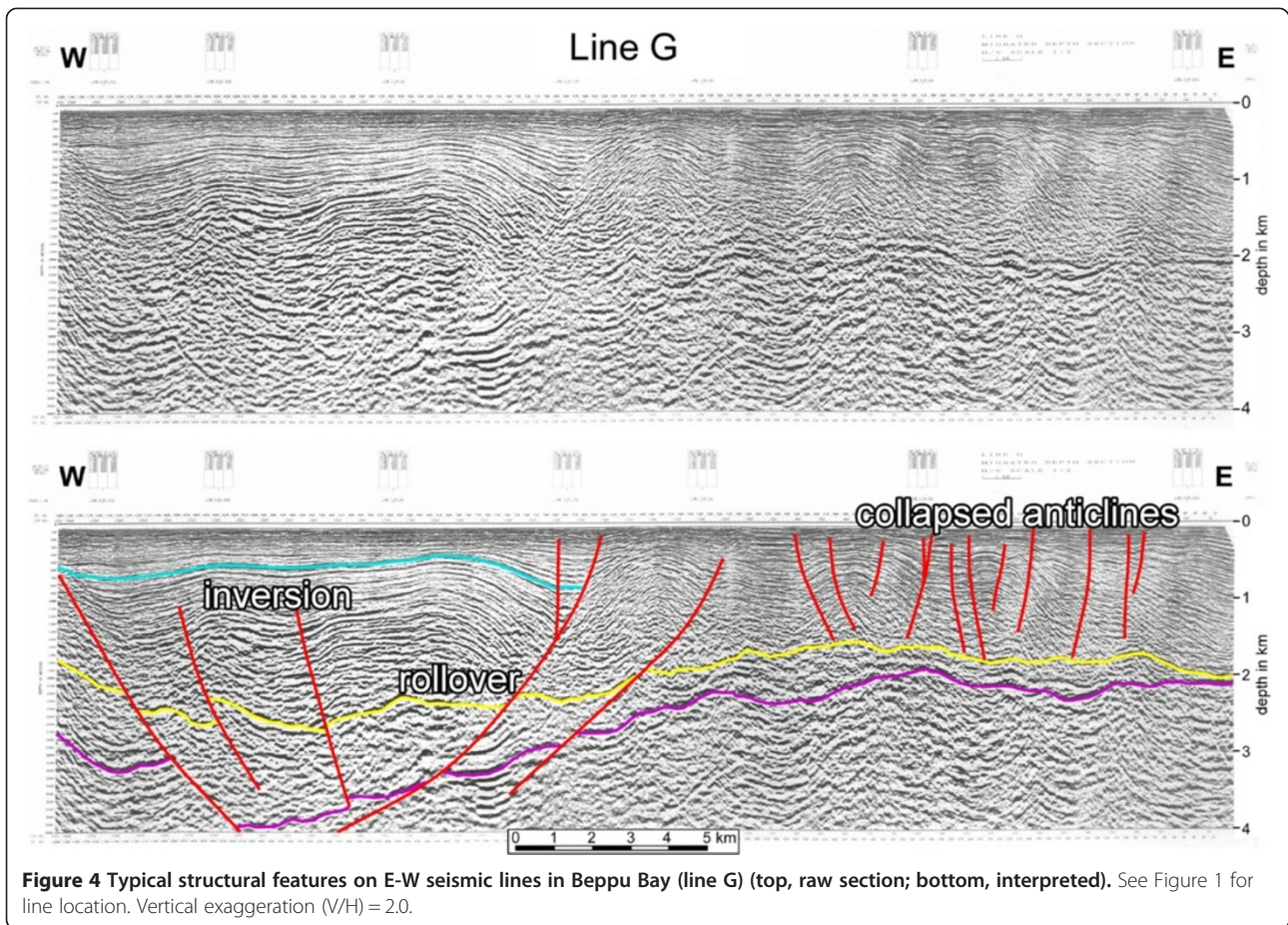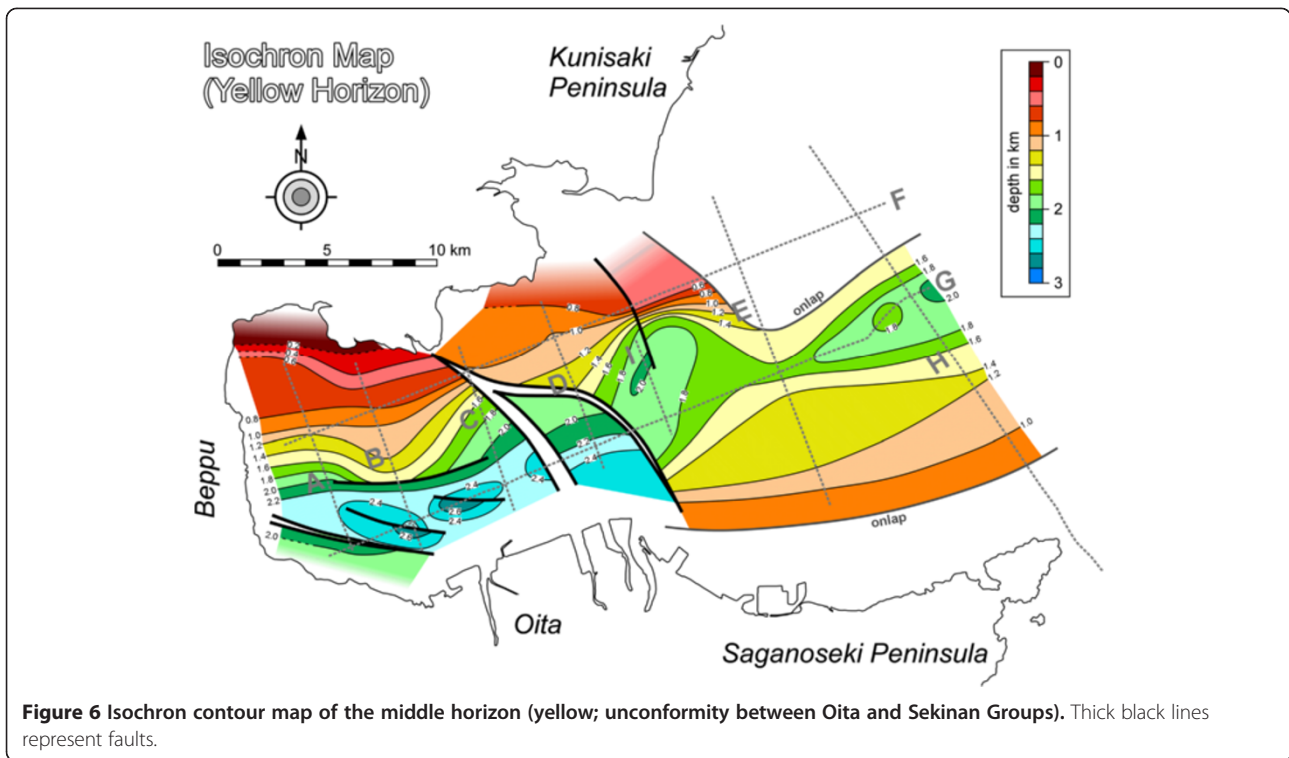
Figure 3 Typical structural features on N-S seismic lines in Beppu Bay (line E) (top, raw section; bottom, interpreted). See Figure 1 for line location. Vertical exaggeration (*V/H*) = 2.0.

the area of the seismic survey was estimated based on basin configuration deduced from gravity anomalies. For Figures 6, 7 the structure beyond our seismic survey area was estimated based on previous shallow seismic data. It is obvious that Beppu Bay is a composite tectonic depression, with the eastern half-graben on the older segment of the MTL and the western pull-apart around a right-stepping portion of the younger MTL (Figure 5). Reflecting changes in tectonic stress, the eastern graben became inactive by the middle of the Quaternary, whereas the western pull-apart continued to develop under enhanced dextral slips on the MTL (Figure 6). The area of active subsidence within the bay has shrunk through the late Quaternary and the recent depocenter is located in the southwestern corner of the bay (Figure 7). An isopach map of Beppu Bay (Figure 8) also delineates two distinct areas of deposition.

Kusumoto et al. (1996) determined a three-dimensional basement structure for the HVZ based on gravimetric data. Itoh et al. (2013b) adopted their elaborate structural model and executed a volumetric analysis of the extensive tectonic depression by means of Gauss-Legendre numerical integration (Davis and Rabinowitz 2007). The volume they estimated for the whole HVZ area was 4.1×10^3 km^3.

Based on current seismic imaging, we attempted to estimate the sediment volumes of the specific periods in Beppu Bay in the same manner. The volumes of the lower and upper units in Beppu Bay were calculated using Gauss-Legendre numerical integration based on depth data for a mesh with 2-km intervals. The volumes for the lower and upper units are 3.1×10^2 and 5.7×10^2 km^3, respectively. The total volume of the Beppu Bay basin since 5 Ma (8.8×10^2 km^3) is about 21% of the HVZ volume.
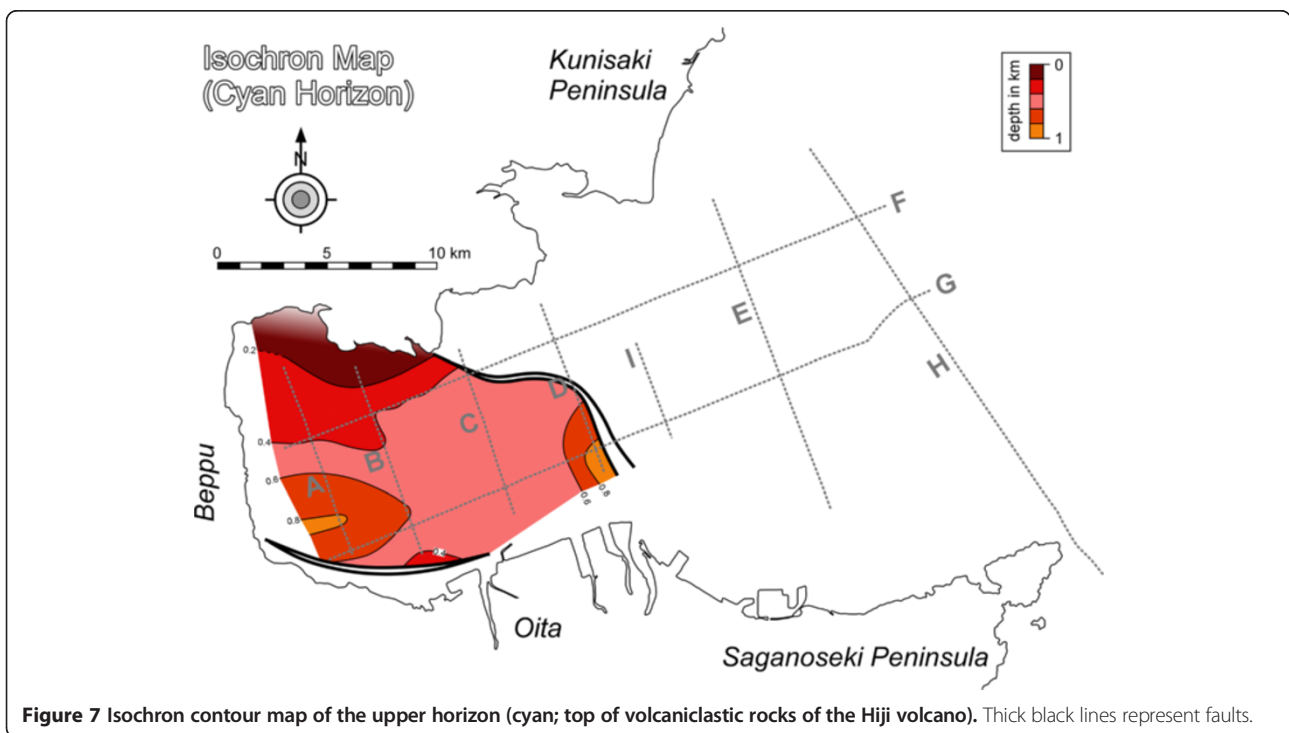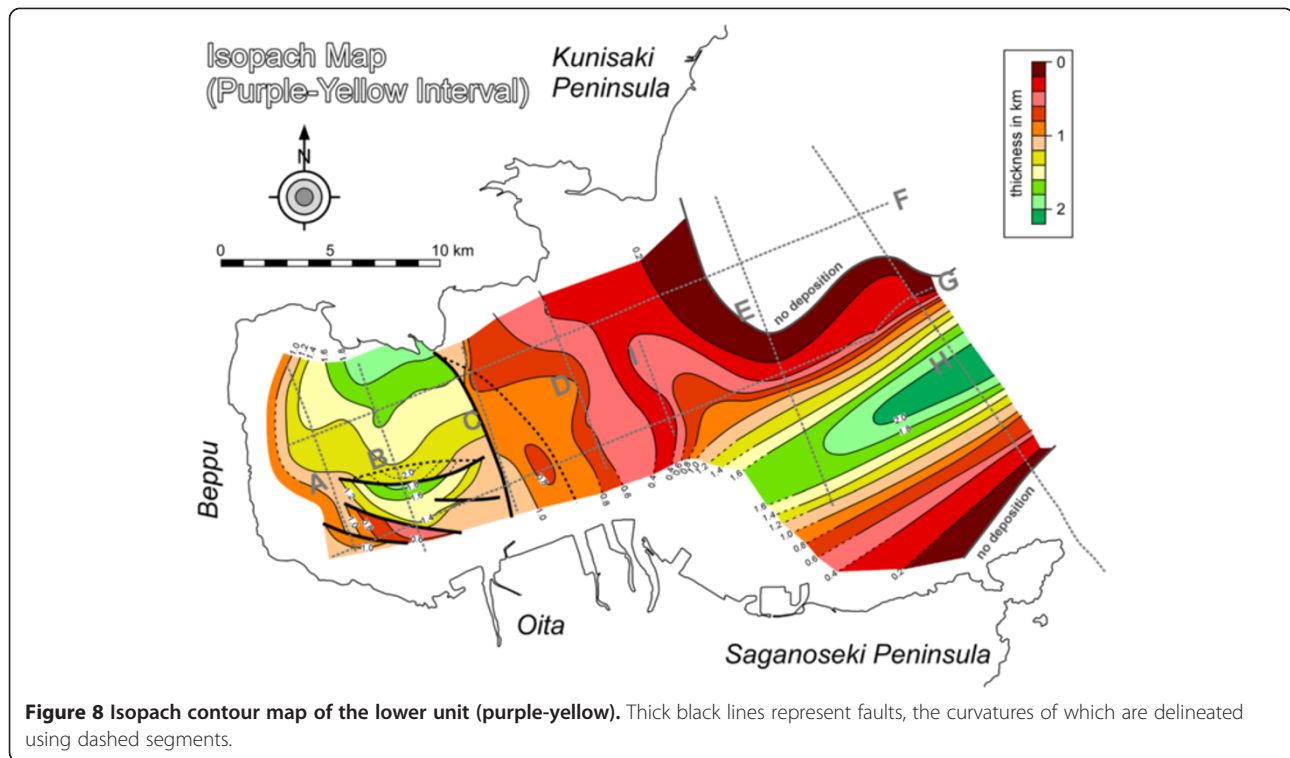
Figure 4 Typical structural features on E-W seismic lines in Beppu Bay (line G) (top, raw section; bottom, interpreted). See Figure 1 for line location. Vertical exaggeration (V/H) = 2.0.

Figure 5 Isochron contour map of the lower horizon (purple; top of acoustic basement). For contour maps, interpretation based on supplementary data (e.g., gravity anomalies, shallow seismic information) is shown by dashed lines. Solid contours were deduced from the present dataset. Thick black lines represent faults.

Figure 6 Isochron contour map of the middle horizon (yellow; unconformity between Oita and Sekinan Groups). Thick black lines represent faults.

Results of seismic survey

The present seismic study revealed that the older asymmetric half-graben on the basal drag fault is thickest along the southern margin of the bay. Figure 3 delineates an irregular surface of the acoustic basement of the

hanging wall (annotated as a 'wedge tip deformation' in the figure). Yusa et al. (1992) and our interpretation indicate that this conspicuous structure is not connected to high-angle faults in upper sedimentary units. Such structural development around the detachment fault is

Figure 7 Isochron contour map of the upper horizon (cyan; top of volcaniclastic rocks of the Hiji volcano). Thick black lines represent faults.

Figure 8 Isopach contour map of the lower unit (purple-yellow). Thick black lines represent faults, the curvatures of which are delineated using dashed segments.

numerically modeled and compared with observed features on seismic profiles in the next 'Discrete element modeling' section.

Spatiotemporal changes in fault activity (transitions of the active MTL segments), migration of the depocenters in Beppu Bay, and emergence of the newly found inversion phase are to be linked to the tectonic regimes on the convergent margin. Such context is examined in the 'Results and discussion' section based on a regional review of tectonic episodes around SWJ.

Discrete element modeling

As shown in Figure 3, the hanging wall of the low-angle detachment at the bottom of the elongate depocenter around the bay mouth, which became dormant in the late Quaternary, shows part of an irregular deformation at the wedge tip. This is not attributed to later disturbance by high-angle faults, because the detachment surface underneath remains intact. It seems that the wedge morphology is controlled by the angle of detachment. Figure 9a presents a high-resolution profile of line J, which runs through the Bungo Strait (Figure 1c). The hanging wall around the survey line has settled on the detachment fault with a steeper angle than on line E and exhibits no remarkable deformation in its wedge tip. We attempted to restore the conspicuous morphology at the basal part of

the tectonic depression with a numerical modeling approach and considered the ancient tectonic framework that provoked the deformation.

Method

We used discrete element modeling to simulate the displacement fields of sedimentary layers caused by normal fault motions of low-angle detachment faults. In the discrete element modeling, media such as crust and/or sedimentary layers are replaced by assemblies of rigid balls (in three-dimensional analyses) or disks (in two-dimensional analyses), connected to each other by imaginary elastic springs in the normal and shear directions. We obtained results such as deformation fields, velocity fields, and other factors by solving the equations for the law of motion and force-displacement law for assemblies under the given conditions.

This modeling procedure was introduced by Cundall (1971) and has been applied to a number of geological and geophysical problems in two and three dimensions (Saltzer and Pollard 1992; Antonellini and Pollard 1995; Strayer and Huddleston 1997; Finch et al. 2003, 2004; Imbera et al. 2004; Vietor and Oncken 2005; Hardy and Finch 2005, 2007; Hardy et al. 2009; Hardy 2011; Yamada et al. 2014). Discrete element modeling has also been applied
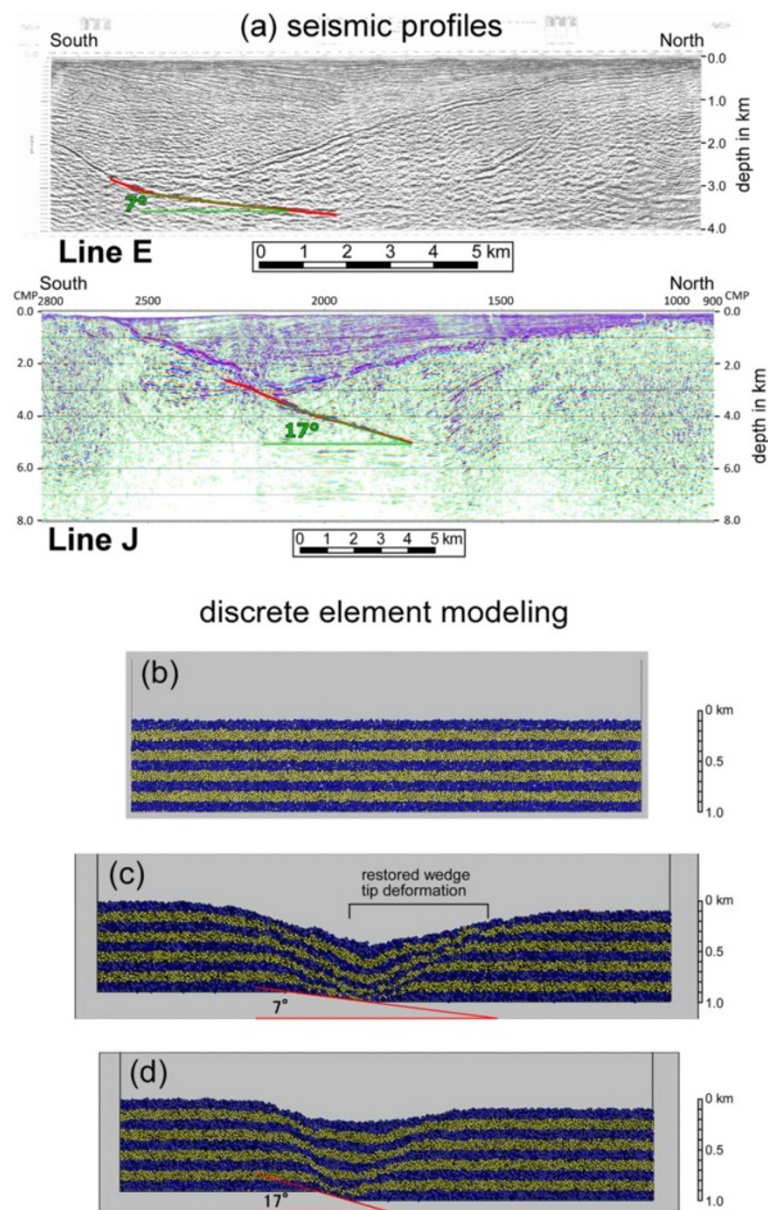
Figure 9 Numerical simulation by means of discrete element modeling. Numerical simulation was performed for restoring structural features within the hanging wall of the low-angle detachment fault. **(a)** Seismic sections (E and J; *V/H* = 1.0) crossing Beppu Bay are shown for reference. The high-resolution profile of line J is after Abe et al. (2013). See Figure 1 for line locations. Detachment faults are delineated by red lines, and measured fault angles are annotated in green. **(b)** Discrete element model of sedimentary layer. The model is 900 m thick and 5,000 m wide. The sedimentary layer is a homogeneous and isotropic medium and is shown in blue and yellow with 100-m interval to identify the displacement field caused by fault motions simply. **(c,d)** Models for actual structure types on different fault angles (Figure 9a). The restored hanging wall deformation in the low-angle model is annotated.

recently in volcanic study fields such as calderas or volcanic depression formations and magma extrusions (e.g., Hardy 2008; Wyrick and Smart 2009; Holohan et al. 2011; Sakai et al. 2013).

In this study, we employed Particle Flow Code in 2 Dimensions (PFC 2D; Itasca 2008) ver. 4.0 software to perform simulations based on the discrete element method.

In the PFC 2D software, the mechanical properties of media are basically determined by the spring constants connecting the disks in the normal and shear directions, the friction coefficient among the disks, and a parameter called the contact bond, which controls the strength of materials. When an actual medium such as crust and/or sedimentary layers is to be modeled using the discrete

Table 1 Modeling parameter values

Parameters	kn [N/m]	ks [N/m]	fric	n_bond [N]	s_bond [N]
Values	5×10^8	5×10^8	0.6	1×10^6	1×10^6

Parameters kn, ks, fric, n_bond, and s_bond are spring constants (stiffnesses) in the normal and shear directions, friction coefficient, and contact bonds in the normal and shear directions, respectively.

element method, we need to carry out biaxial tests in the computer because of the necessary two-dimensional analyses to decide upon the values of these parameters, arriving at the elastic constants and strength we want by trial and error. In general, motions of particles will be slower for larger spring constants. We refer to this characteristic and changed the mechanical properties of the media by varying the combinations of the spring constants in the normal and shear directions.

Results

Since the sediments that have accumulated in Beppu Bay are young and have been laid on a shallow sea bottom, we assumed that they are unconsolidated sediments and have low Young's moduli and strengths. In the numerical simulations, we assigned the values shown in Table 1 to the spring constants, friction coefficient, and contact bond. These parameter values were determined by trial and error, as noted above, to obtain a low Young's modulus and strength. The medium, consisting of assemblies of disks having these parameters, is equivalent to the sediment layer having a Young's modulus, Poisson's ratio, and compressive strength of 207 MPa, 0.24, and 13 MPa, respectively. These elastic constants and strength compare to values shown in some textbooks (e.g., Cernica, 1995; Budhu, 2007; Gudmundsson, 2011). The model of the sediment layer is 900 m thick and 5,000 m wide and is colored blue and yellow with 100-m intervals to display the displacement fields caused by fault motions easily (Figure 9b). The basement and both sides of the model are rigid walls and can move somewhat without changing their shapes as general deformation of the basement layer caused by motion of the detachment fault. The density of the elements was assumed to be 2,000 kg/m^3 (cf. Kusumoto et al. 1996), and a gravitational body force was assigned to each element during the calculations.

In Figures 9c,d, we show displacement fields for the sedimentary layer simulated by motions of the detachment fault having a dip angle of 7° for line E and 17° for line J. These dip angles were estimated from reflection structures shown in the seismic profiles (Figure 9a). In the simulations, normal fault motions were given on the fault plane by iterative calculations until the accumulated vertical displacement reached 100 m. The numerical simulations (cf. 'restored wedge tip deformation' in Figure 9c) are very similar to the characteristic structures shown

in the seismic profiles (like the irregularity of the surface structure of the hanging wall) and indicate that structural differences in the deformed sedimentary layer are caused by differences in the dip angles of the faults.

These results suggest that the activity of a low-angle detachment simultaneously causes obscuration of stratifications in the deformed hanging wall under specific conditions, which may be misinterpreted as successive development of minor faults under different tectonic regimes. Numerical modeling can, thus, be incorporated into structural restoration and support the validity of geologic interpretation. A strong N-S tensional regime confirmed in the incipient stage of basin formation was not restricted to Beppu Bay, but was a regional phenomenon at the beginning of the Pliocene. Because our seismic and modeling results have clarified the time sequence of the tectonic regimes, we can submit a neotectonic synthesis of SWJ under the influence of oblique subduction of an oceanic plate.

Results and discussion

Seismic data have revealed the structural features of a large tectonic depression around Beppu Bay. Its complicated evolutionary process records the transitions of tectonic stress on the Philippine Sea plate convergent margin. Generally speaking, regional uplift/subsidence trends around an island arc are closely connected with subduction of an oceanic plate. Hashimoto et al. (2008) successfully restored geomorphological features and free-air gravity anomalies around northeast Japan based on elastic/viscoelastic dislocation theory. They assumed a long steady subduction of the Pacific plate and an episode of tectonic erosion since 3 ~ 4 Ma to optimize the numerical model.

SWJ has been under the influence of the Philippine Sea plate convergence and is characterized by more complicated deformation patterns. In the following sections, the authors present a chronicle of remarkable episodes around SWJ since 6 Ma, when a tectonically dormant period after the backarc opening in the Japan Sea was replaced by intensive tectonism. We submit a working hypothesis of transient plate subduction. Throughout our examination, structural development around the Beppu Bay provides important clues for solving the sequence of tectonic events.

Nakamura et al. (1987) first advocated a recent jump of the Euler pole of the Philippine Sea plate based on structural features near the subduction zone around eastern SWJ. We submit the hypothesis that older events of the Euler pole jump may better explain the spatiotemporal transition of tectonic stress along the island arc.
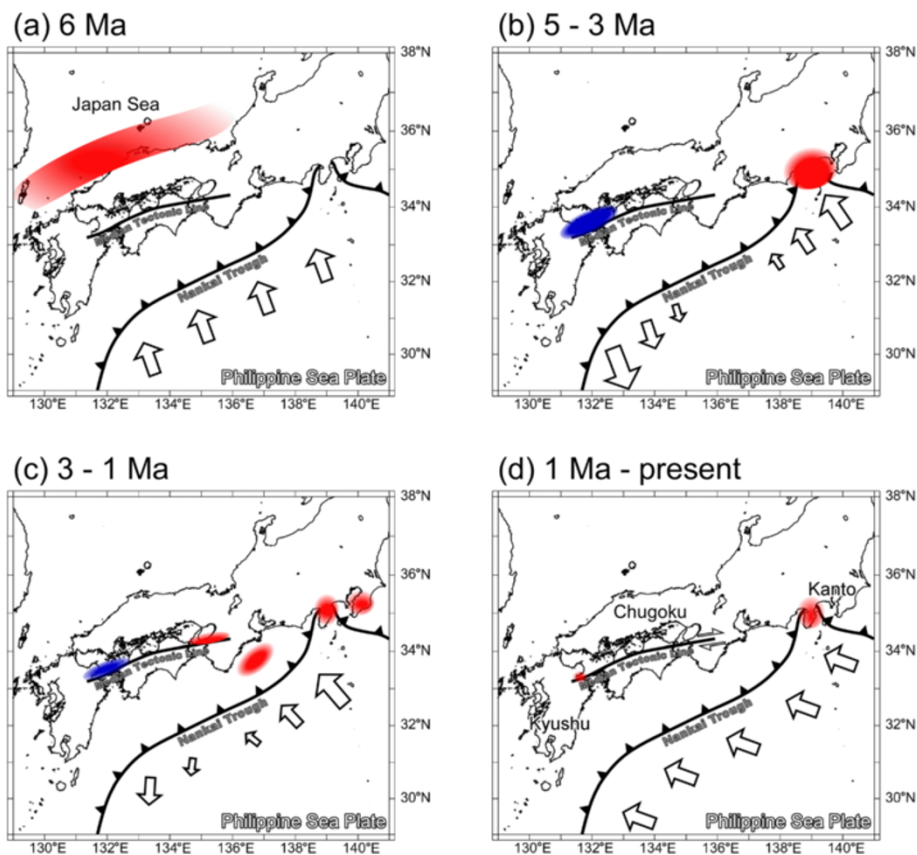
Figure 10 Spatiotemporal distribution of stress-strain regime in southwest Japan and kinematic model of the Philippine Sea/Eurasian plate convergence. Red and blue portions represent areas of compressive (contractional) and tensile (extensional) stress (strain), respectively. Modes of the Philippine Sea plate convergence are schematically shown by the length and azimuth of the arrows. **(a,b,c,d)** Sequential tectonic epochs of SWJ since 6 Ma, which are described in the text.

Regional contraction along the SWJ backarc (ca. 6 Ma)

Around SWJ, one of the most noted tectonic events in the late Cenozoic is a remarkable N-S backarc contraction. It was originally described by Tai (1973) based on structural trends in the Japan Sea coastal area. Utilizing seismic reflection data, Itoh and Nagasaki (1996) clarified that the deformation zone covers the entire backarc shelf. Its western termination merged into the marginal fault of the Japan Sea and reactivated it in the opposite (sinistral) sense to its initial dextral activity during the Miocene backarc opening (Itoh 2001). Although the activity level seems to diminish eastward, Itoh et al. (1997, 2006) showed a coeval deformation on the eastern SWJ backarc. If the regional event is linked with oceanic plate motion, the Philippine Sea plate probably imposed a northerly convergence at ca. 6 Ma (Figure 10a).

Basin development related to lopsided convergence (5 ~ 3 Ma)

In contrast to the preceding stage, the early Pliocene is characterized by the emergence of an enormous area of extension and basin formation around the western part of the MTL, including Beppu Bay (Itoh et al. 2013a, b). As summarized by Itoh et al. (1998), N-S tensile stress was dominant around the western part of SWJ. On the other hand, the eastern part of SWJ was a site of strong compression, accompanied by the collision of the Tanzawa landmass (Niitsuma 1999) against the eastern forearc. Between the disturbed ends of the island arc, the central part of SWJ was free from strong deformation, and basin formation was inactive throughout the period (Figure 10b). Similar stress variations along the active trace of the MTL were pointed out by Ikeda et al. (2009). Although they attributed the deformation mode to counterclockwise motion of the forearc sliver relative to the mother continent based on GPS observations (Nishimura and Hashimoto 2006), our geologic review has shown that larger areas were involved in the tectonic episode implying more regional motive force. We assume that such a tectonic trend is related to lopsided subsidence, namely a jump of the Euler pole of the Philippine Sea/Eurasian plates.

Expansion of the contractional domain (3 ~ 1 Ma)

The early Quaternary was an era of contractional deformation around SWJ. The eastern part of the arc was under a continued compressive regime, which provoked formation of a regional unconformity in the eastern forearc around 3.0 ~ 2.5 Ma (e.g., Kameo et al. 2010; Kameo and Sekine 2013). Watershed mountains simultaneously emerged along the MTL in the central part of SWJ (Oka 1978; Oka and Sangawa 1981; Mizuno 1987), which was succeeded by extensive deformation of the adjoining forearc basin (Takano et al. 2009). As depicted in the isochron map of the yellow horizon (Figure 6), the tension graben around Beppu Bay in the western part of the island arc became inactive and the basin architecture changed to be under a transtensional/transpressional regime. Such tectonic features (Figure 10c) may be related to continued migration of the Euler pole of the Philippine Sea plate.

Dominance of simple shear deformation (1 Ma ~ present)

The latest change in the convergence mode is thought to have occurred around 1 ~ 2 Ma. Nakamura et al. (1987) described the submarine topography and shallow structure along the eastern forearc slope of SWJ and advocated a counterclockwise shift (north-northwestward to west-northwestward) of the convergent direction of the Philippine Sea plate. Cessation of uplift of the watershed mountain ranges (Oka 1978) and dominance of simple shear deformation (Itoh and Takemura 1993) of mid-SWJ are concordant with such a tectonic event. A change in the plate motion around 1 Ma is also supported by structural analysis of the convergent margin to the east of Kyushu Island (Yamazaki and Okamura 1989). In front of the thrusting forearc sliver and subducting oceanic plate, Kyushu has been a site of lateral extrusion (Itoh and Takemura 1994) and vigorous arc volcanism (e.g., Nakada and Kamata 1991; Kamata et al. 1994). Thus, the present convergence mode between the Eurasian/Philippine Sea plates (Figure 10d) is regarded as the latest temporal fluctuation.

Enhanced dextral motion on the MTL caused by the accelerated oblique subduction has resulted in the recent development of flower structures and the active subsidence of a pull-apart basin in the Beppu Bay. The tectonic epoch of the HVZ is expressed as a regional unconformity on land and a conspicuous reflector (Yellow horizon) in the bay at 0.7 Ma. As described in 'Structural interpretation and volumetric analysis' section, the volume of the Beppu Bay sediments above the horizon is nearly double that of the lower unit, indicating a vigorous pull-apart formation in a rather short period.

Conclusions

The authors recognized and traced conspicuous intra-basin seismic reflectors around Beppu Bay, in the westernmost part of SWJ. Detailed analyses of the seismic data revealed the following stratigraphic, structural, and neotectonic features in the study area that are closely related to regional tectonic regimes around SWJ.

1. Beppu Bay, located in the western portion of the arc-bisecting dextral fault (MTL), is a tectonic depression existing since ca. 5 Ma. Sediments burying the basin are divided into lower (5 ~ 0.7 Ma), upper (0.7 ~ 0.3 Ma), and an auxiliary uppermost (0.3 Ma ~ present) units in ascending order.

2. Major subsurface structures in Beppu Bay are an older half-graben under strong N-S extensional regime and a younger pull-apart sag that developed in a right-stepping part of the MTL as a result of increased late Quaternary strike-slip rates on the fault. Unconsolidated sediments within the pull-apart are deformed by later inversion events. The subsidence rate of the long-standing tectonic depression has been diminishing as contraction arose.

3. Conspicuous syn-faulting deformation of the hanging wall of the low-angle detachment in the deep basin interior was successfully reproduced by numerical simulations. Based on a discrete element method, this suggests that structural differences in the deformed wedge are caused by differences in the dip angles of the detachment faults and that the study area was under strong N-S tensional stress through the early stage of basin formation.

4. Remarkable temporal changes in the tectonic regimes around Beppu Bay and other areas along the island arc are probably related to transient modes of convergence of the Philippine Sea plate since ca. 6 Ma.

Author details
[1]Graduate School of Science, Osaka Prefecture University, Osaka 599-8531, Japan. [2]Graduate School of Science and Engineering for Research, University of Toyama, Toyama 930-8555, Japan. [3]Graduate School of Science, Kyoto University, Kyoto 606-8502, Japan.

References

Abe S, Niiro R, Ino S (2013) Hybrid optimization for prediction and suppression of long-period multiples. In: (ed) Abstracts of the 128th conference of the Society of Exploration Geophysicists of Japan

Antonellini MA, Pollard DD (1995) Distinct element modelling of deformation bands in sandstone. J Struct Geol 17:1165–1182

Budhu N (2007) Soil mechanics and foundations, 2nd edn. Wiley, New York

Cernica JN (1995) Geotechnical engineering soil mechanics. Wiley, New York

Cundall PA (1971) A computer model for simulating progressive large scale movements in blocky rock systems. In: (ed) Proceedings of symposium for International Society of Rock Mechanics, 1, Paper No. Il-8

Davis PJ, Rabinowitz P (2007) Methods of numerical integration, 2nd edn. Dover, New York

Finch E, Hardy S, Gawthorpe RL (2003) Discrete element modelling of contractional fault-propagation folding above rigid basement blocks. J Struct Geol 25:515–528

Finch E, Hardy S, Gawthorpe RL (2004) Discrete element modelling of extensional fault-propagation folding above rigid basement fault blocks. Basin Res 16:489–506

Gudmundsson A (2011) Rock fractures in geological processes. Cambridge University Press, London

Harding TP (1990) Identification of wrench faults using subsurface structural data: criteria and pitfalls. AAPG Bull 74:1590–1609

Hardy S (2008) Structural evolution of calderas: insights from two-dimensional discrete element simulations. Geology 36:927–930, doi:10.1130/G25133A.1

Hardy S (2011) Cover deformation above steep, basement normal faults: insights from 2D discrete element modeling. Mar Petrol Geol 28:966–972

Hardy S, Finch E (2005) Discrete-element modelling of detachment folding. Basin Res 17:507–520, doi:10.1111/j.1365-2117.2005.00280.x

Hardy S, Finch E (2007) Mechanical stratigraphy and the transition from trishear to kink-band fault-propagation fold forms above blind basement thrust faults: a discrete-element study. Mar Petrol Geol 24:75–90

Hardy S, McClay K, Muñoz JA (2009) Deformation and fault activity in space and time in high-resolution numerical models of doubly vergent thrust wedges. Mar Petrol Geol 26:232–248, doi:10.1016/j.marpetgeo.2007.12.003

Hashimoto C, Sato T, Matsu'ura M (2008) 3-D simulation of steady plate subduction with tectonic erosion: current crustal uplift and free-air gravity anomaly in northeast Japan. Pure Applied Geophys 165:567–583, doi:10.1007/s00024-008-0321-0

Holohan EP, Schöpfer MPJ, Walsh JJ (2011) Mechanical and geometric controls on the structural evolution of pit crater and caldera subsidence. J Geophys Res 116, B07202, doi:10.1029/2010JB008032

Ikeda M, Toda S, Kobayashi S, Ohno Y, Nishizaka N, Ohno I (2009) Tectonic model and fault segmentation of the Median Tectonic Line active fault system on Shikoku, Japan. Tectonics 28, TC5006, doi:10.1029/2008TC002349

Imbera J, Tuckwell GW, Childs C, Walsh JJ, Manzocchi T, Heath AE, Bonson CG, Strand J (2004) Three-dimensional distinct element modelling of relay growth and breaching along normal faults. J Struct Geol 26:1897–1911

Ishizuka Y, Mizuno K, Matsuura H, Hoshizumi H (2005) Geology of the Bungo-Kitsuki district. Quadrangle Series, 1:50,000. Geological Survey of Japan, AIST, Tsukuba

Itasca (2008) PFC2D - Particle Flow Code in 2 Dimensions, ver. 4.0. Itasca Consulting Group Inc, Minneapolis, Minnesota

Itoh Y (2001) A Miocene pull-apart deformation zone at the western margin of the Japan Sea back-arc basin: implications for the back-arc opening mode. Tectonophysics 334:235–244

Itoh Y (2013) Mechanism of sedimentary basin formation - multidisciplinary approach on active plate margins. InTech, Rijeka (Croatia), http://dx.doi.org/10.5772/50016

Itoh Y, Nagasaki Y (1996) Crustal shortening of Southwest Japan in the Late Miocene. Island Arc 5:337–353

Itoh Y, Takemura K (1993) Quaternary geomorphic trends within Southwest Japan: extensive wrench deformation related to transcurrent motions of the Median Tectonic Line. Tectonophysics 227:95–104

Itoh Y, Takemura K (1994) Mode of Quaternary crustal deformation of Kyushu Island, Japan. In: Shichi R, Heki K, Kasahara M, Kawasaki I, Murakami M, Nakahori Y, Okada K, Okubo S, Ota Y, Takemoto S (eds) Proceedings of 8th international symposium on recent crustal movements. The Local Organizing Committee for the CRCM'93, Kyoto

Itoh Y, Takemura K, Kusumoto S (2013a) Neotectonic intra-arc basins within Southwest Japan - conspicuous basin-forming process related to differential motion of crustal blocks. In: Itoh Y (ed) Mechanism of sedimentary basin formation - multidisciplinary approach on active plate margins. InTech, Rijeka (Croatia), http://dx.doi.org/10.5772/56588

Itoh Y, Kusumoto S, Takemura K (2013b) Characteristic basin formation at terminations of a large transcurrent fault - basin configuration based on gravity and geomagnetic data. In: Itoh Y (ed) Mechanism of sedimentary basin formation - multidisciplinary approach on active plate margins. InTech, Rijeka (Croatia), http://dx.doi.org/10.5772/56702

Itoh Y, Nakajima T, Takemura A (1997) Neogene deformation of the back-arc shelf of Southwest Japan and its impact on the palaeoenvironments of the Japan Sea. Tectonophysics 281:71–82

Itoh Y, Takemura K, Kamata H (1998) History of basin formation and tectonic evolution at the termination of a large transcurrent fault system: deformation mode of central Kyushu, Japan. Tectonophysics 284:135–150

Itoh Y, Uno K, Arato H (2006) Seismic evidence of divergent rifting and subsequent deformation in the southern Japan Sea, and a Cenozoic tectonic synthesis of the eastern Eurasian margin. J Asian Earth Sci 27:933–942

Itoh Y, Takano O, Kusumoto S, Tamaki M (2014) Mechanism of long-standing Cenozoic basin formation in central Hokkaido: an integrated basin study on an oblique convergent margin. Prog Earth Planet Sci 1:6, http://www.progearthplanetsci.com/content/1/1/6

Kamata H (1989) Volcanic and structural history of the Hohi volcanic zone, central Kyushu, Japan. Bull Volcanol 51:315–332

Kamata H, Danhara T, Hayashida A, Hoshizumi H, Yamashita T (1994) Correlation of the Imaichi pyroclastic-flow deposit to the similar pyroclastic-flow deposits in central Kyushu, Japan, and estimation of their source vent. J Geol Soc Jpn 100:279–291

Kamata H, Uto K, Uchiumi S (1988) Geochronology and evolution of the post-Shishimuta caldera activity around the Waitasan area in the Hohi volcanic zone, Kyushu, Japan. Bull Volcanol Soc Jpn 33:305–320

Kameo K, Sekine T (2013) Calcareous nannofossil biostratigraphy and the geologic age of the Anno Formation, the Awa Group, in the Boso Peninsula, central Japan. J Geol Soc Jpn 119:410–420

Kameo K, Shindo R, Takayama T (2010) Calcareous nannofossil biostratigraphy and geologic age of the Kiyosumi Formation of the Awa Group, Boso Peninsula, central Japan: age determination based on size variations of *Reticulofenestra* specimens. J Geol Soc Jpn 116:563–574

Komazawa M (2004) Gravity grid database of Japan, Gravity CD-ROM of Japan, ver. 2, Digital Geoscience Map P-2. Geol Surv Jpn Tsukuba

Kusumoto S, Fukuda Y, Takemura K, Yusa Y (1996) Three-dimensional subsurface structure in the eastern part of the Beppu-Shimabara Graben Kyushu, Japan, as revealed by gravimetric data. J Geod Soc Jpn 42:167–181

Kusumoto S, Takemura K, Fukuda Y, Takemoto S (1999) Restoration of the depression structure at the eastern part of central Kyushu, Japan by means of dislocation modeling. Tectonophysics 302:287–296

Mizuno K (1987) Preliminary report on the Plio-Pleistocene sediments distributed along the Median Tectonic Line in and around Shikoku, Japan. Bull Geol Surv Jpn 38:171–190

Nakada S, Kamata H (1991) Temporal change in chemistry of magma source under central Kyushu, southwest Japan: progressive contamination of mantle wedge. Bull Volcanol 53:182–194

Nakamura K, Renard V, Angelier J, Azema J, Bourgois J, Deplus C, Fujioka K, Hamano Y, Huchon P, Kinoshita H, Labaume P, Ogawa Y, Seno T, Takeuchi A, Tanahashi M, Uchiyama A, Vigneresse JL (1987) Oblique and near collision subduction, Sagami and Suruga Troughs - preliminary results of the French-Japanese 1984 Kaiko cruise, Leg 2. Earth Planet Sci Lett 83:229–242

Niitsuma N (1999) Rupture and delamination of arc crust rupture and delamination of island arc crust due to the arc-arc collision in the South Fossa Magna, central Japan. Island Arc 8:441–458

Nishimura S, Hashimoto M (2006) A model with rigid rotations and slip deficits for the GPS-derived velocity field in Southwest Japan. Tectonophysics 421:187–207

Oka Y (1978) The formation of the Izumi Range and the Osaka Group. Quat Res 16:201–210

Oka Y, Sangawa A (1981) The formation of the sedimentary basin in the east of Inland Sea and the uplift of the Awaji Island, Japan. J Geogr 90:393–409

Research Group for Active Faults (1991) The active faults in Japan: sheet maps and inventories, revised edition. University of Tokyo Press, Tokyo

Sakai N, Kusumoto S, Shimizu Y (2013) Numerical simulations of middle-high viscous magma extrusion by means of discrete element modeling. Bull Volcanol Soc Jpn 58:551–555

Saltzer SD, Pollard DD (1992) Distinct element modeling of structures formed in sedimentary overburden by extensional reactivation of basement normal faults. Tectonics 11:165–174

Sasada M (1987) Pre-Tertiary basement rocks of Hohi area, central Kyushu, Japan. Bull Geol Surv Jpn 38:385–422

Strayer LM, Huddleston PJ (1997) Numerical modelling of fold initiation at thrust ramps. J Struct Geol 19:551–566

Tai Y (1973) On the 'Shinji folded zone'. Mem Geol Soc Jpn 9:137–146

Takano O, Itoh Y, Kusumoto S (2013) Variation in forearc basin configuration and basin-filling depositional systems as a function of trench slope break development and strike-slip movement: examples from the Cenozoic Ishikari - Sanriku-Oki and Tokai-Oki - Kumano-Nada Forearc Basins, Japan. In: Itoh Y (ed) Mechanism of sedimentary basin formation - multidisciplinary approach on active plate margins. InTech, Rijeka (Croatia), http://dx.doi.org/10.5772/56751

Takano O, Nishimura M, Fujii T, Saeki T (2009) Sequence stratigraphic distribution analysis of methane-hydrate-bearing submarine-fan turbidite sandstones in the eastern Nankai Trough area: relationship between turbidite facies distributions and BSR occurrence. J Geogr 118:776–792

Vietor T, Oncken O (2005) Controls on the shape and kinematics of the Central Andean plateau flanks: insights from numerical modeling. Earth Planet Sci Lett 236:814–827, doi:10.1016/j.epsl.2005.06.004

Wyrick DY, Smart KJ (2009) Dike-induced deformation and Martian graben systems. J Volcanol Geotherm Res 185:1–11, doi:10.1016/j.jvolgeores.2008.11.022

Yamada Y, Baba K, Miyakawa A, Matsuoka T (2014) Granular experiments of thrust wedges: insights relevant to methane hydrate exploration at the Nankai accretionary prism. Mar Petrol Geol 51:34–48, doi:10.1016/j.marpetgeo.2013.11.008

Yamazaki T, Okamura Y (1989) Subducting seamounts and deformation of overriding forearc wedges around Japan. Tectonophysics 160:207–229

Yusa Y, Takemura K, Kitaoka K, Kamiyama K, Horie S, Nakagawa I, Kobayashi Y, Kubotera A, Sudo Y, Ikawa T, Asada M (1992) Subsurface structure of Beppu Bay (Kyushu, Japan) by seismic reflection and gravity survey. Zisin (Bull Seismol Soc Jpn) 45:199–212